

Student Name: Conrad Goerz

Date: August 7/2015

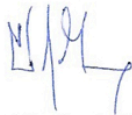
Project Title: Centrosomal Protein of 55 kDa (CEP55): Expression and localization in human brain development

Primary Supervisor Name :
Dr. Marc Del Bigio, Neuropathology

Department:
Dr. Kant Matsuda, Neuropathology

SUMMARY: (no more than 250 words single spaced)

Hydranencephaly is an uncommon congenital anomaly defined as a near complete absence of the cerebral hemispheres, replacement of the missing neural tissue with fluid-filled sacs, and relative preservation of the posterior fossa structures. A rare syndrome with hydranencephaly, dysplastic kidneys and polysyndactyly was described in three children from the same family of Mennonite ancestry by Dr. P. Frosk in the Department of Medical Genetics at the University of Manitoba. This constellation of anomalies has only been described rarely. Genetic analysis showed that they were homozygous for a mutation in the Centrosomal Protein of 55 kDa (CEP55) gene; the protein is an important regulator in cytokinesis (the final stage of cell division after mitosis) of cells. Interrogation of a gene expression database (BrainSpan) showed that regions with high CEP55 mRNA expression have more destruction and those brain regions with lower CEP55 mRNA expression had multinucleate cells. Using immunohistochemical methods in human brain tissue spanning the age spectrum, as well as control kidney tissue and brain tissue from affected cases, we found that all brain tissue has high cytoplasmic CEP55 expression during early development. CEP55 immunostaining in control and homozygous tissue localized to the proliferative external granular zone of the cerebellum, the neocortical region, the ventricular zone, and superficial region of the subventricular zone of the ganglionic eminence, and tubule cells in normal kidney. These data support CEP55 as the causative mutation in human brain maldevelopment, although protein expression into adulthood indicate a role other than or in addition to cytokinesis.



Student Signature



Supervisor Signature

ACKNOWLEDGEMENTS:

I gratefully acknowledge the support by one or more of the following sponsors;

CancerCare MB

H.T. Thorlakson Foundation

Dean, College of Medicine

Research Manitoba

Children's Hospital Research Institute of MB

Kidney Foundation of Manitoba

Manitoba Medical Service Foundation

Associate Dean (Research), College of

Medicine

Heart and Stroke Foundation

Health Sciences Centre Research

Foundation

Other:

Introduction and Background

Hydranencephaly is an uncommon congenital anomaly with a frequency of approximately 1 in 10,000 births.(1) Conflicting definitions in the literature make it difficult to compare case reports. However, the most current and concrete definition of hydranencephaly is a near complete absence of the cerebral hemispheres, replacement of the missing neural tissue with fluid-filled sacs, relative preservation of the posterior fossa structures, and a normal cranial compartment. Thus, as opposed to extreme hydrocephalus (in which the ventricles in the head expand and white matter damage occurs secondarily), hydranencephaly incorporates a destructive component that involves the cerebral cortex. It can be diagnosed prenatally and be differentiated from hydrocephalus through fetal MRI or with postnatal imaging. It can occur as an isolated anomaly or as part of a syndrome. Underlying associations include teratogens (e.g. congenital infections, valproic acid exposure), chromosomal disorders (e.g. trisomy 13, triploidy), and single gene disorders (e.g. proliferative vasculopathy, X-linked hydranencephaly with abnormal genitalia).(2,3) The pathophysiology in the majority of cases of hydranencephaly is thought to be early fetal intracranial vascular obstruction that leads to necrosis and cystic degeneration of the cerebral hemispheres.(3)

A rare condition was described in three fetuses from the same family of Dutch-German Mennonite ancestry by Dr. Patrick Frosk in the Department of Medical Genetics at the University of Manitoba (unpublished). Ultrasound examination in utero showed oligohydramnios, small dysplastic kidneys, and extensive brain destruction with enlargement of the cerebral ventricles, consistent with hydranencephaly. All three were stillborn in the third trimester and underwent autopsy. External examination of all three showed microretrognathia, epicanthal folds and pinched nose with a bulbous tip. The upper limbs had limb contractures, with broad hands, single transverse palmar creases and fifth finger clinodactyly. Talipes equinovarus, prominent syndactyly of the toes and a very wide first web space of the toes was present in the lower limbs. Autopsy examination showed small dysplastic aortic valves, dilated and fibrotic left ventricles, severe pulmonary hypoplasia, and only vestigial remnants of renal tissue. The cerebellum, brain stem, basal nuclei, and regions of the temporal and frontal lobes were hypoplastic with multinucleated neurons. The remainder of the cerebrum was either missing or reduced to islands of tissue. No evidence of infection, inflammation, or vascular obstruction could be identified.

An extensive literature search revealed nine similar cases with hydranencephaly, renal dysplasia, and syndactyly.(4–8) All had hydranencephaly, and eight of the nine had renal aplasia or severe renal dysplasia. One child had functioning kidneys, given that he survived for more than one month, but it is not clear whether there was some element of renal dysplasia since he was not investigated in this respect.(6) He likely has the same disorder given that his sister had the full phenotype. In none of the case reports had a genetic cause been identified. Where neuropathology was done, multinucleated neurons were frequently described.(4,5,8) Of the nine cases, two were singletons and seven were from families with multiple affected children. Three of the nine cases were female.

Combined with the Manitoba family, this is highly suggestive of an autosomal recessive etiology, particularly in view of the fact that the Manitoba family is from a population with a relatively strong founder effect.(9)

Genetic analysis of the affected Manitoba family showed that the affected fetuses were all homozygous for two genetic mutations, one of which was excluded because there was no amino acid change. The candidate mutation was a homozygous mutation in the *CEP55* (Centrosomal Protein of 55 kDa) gene (rs201430235, c.1274C>A, p.S425X [NM_001127182]). This variant has been previously identified through a large-scale variant identification project in two separate individuals, both of whom were heterozygous (http://genome.sph.umich.edu/wiki/Exome_Chip-Design). The project classifies this mutation as “extremely rare” with an estimated allele frequency of 0.02% (2 heterozygotes out of 5,000 exome sequences). The variant occurs in the final exon of the gene and the predicted effect is truncation of the C-terminal 40 amino acids given that the aberrant mRNA would likely escape the effects of nonsense mediated decay.(10) Sanger sequencing of the family showed that the parents were heterozygotes for the mutation and an additional sibling was heterozygous for the mutation.

CEP55 is a nine exon gene found at chromosome 10.23.33. It encodes CEP55, a 464 amino acid protein containing three central coiled-coil domains. Research has shown an association between the CEP55 protein and the centriole, with the protein acting as an important regulator of cytokinesis (the final stage of cell division after mitosis) in cells.(11) In the adult, CEP55 is expressed at high levels in the thymus, testis and bone marrow and at basal levels in other tissues including brain.(12) It is localized to the centrosome and pericentriolar matrix during most of the cell cycle, but diffuses throughout the cell at the onset of mitosis (prophase) while the centrioles are separating and chromatin condensation is taking place.(12) As mitosis progresses, it migrates towards the spindle midzone. During cytokinesis it is strongly concentrated in the midbody, the protein complex present in the cytoplasmic bridge between the two daughter cells.(12) The midbody is the intercellular bridge that connects the two dividing cells.

While in the midbody, CEP55 is instrumental in recruiting the Endosome Sorting Complex Required for Transport (ESCRT) as well as providing a scaffold for other anchoring proteins. In this capacity, CEP55 acts to promote the formation of the cleavage furrow and eventually induces abscission of the two cells.(13) The initial disassociation of CEP55 from the centriole appears to be entirely dependent on phosphorylation of the two C-terminal residues, S425 and S428, by the protein kinases Erk2 and Cdk1.(14) Subsequent to this, another protein kinase, Plk1, phosphorylates S436 which stabilizes the protein and eventually leads to its orderly introduction into the midbody.(12,15,16) If either of these events does not occur, then cytokinesis and cell abscission fail despite successful mitosis. This results in a binucleate cell. Cytokinetic failure has been shown to result from both knocking out *CEP55* expression and by mutating either S425/S428 or S436 so they cannot be phosphorylated.(12,14,17) Additionally, CEP55 is integral for the degradation of midbody remnants post-cytokinesis. Depletion of CEP55 results in the accumulation of midbody remnants, which is associated with stem-cell like properties and tumourgenicity.(18)

To date, no mutations in *CEP55* have been associated with human disease and most research on this gene and its corresponding protein has focused on its role in cytokinesis. CEP55 has also been linked with tumourigenesis and metastases. In breast cancer increased expression of CEP55 is associated with metastasis and a poorer prognosis.(19)

Despite an exhaustive search, we were unable to find any published work on the specific role of CEP55 protein at different stages of development in the human brain or any other organ system. The goal of this project is to further characterize the localization of the CEP55 protein in normal brain tissue and brain tissue from individuals with a *CEP55* mutation. Hopefully this will further elucidate the pathogenesis of hydranencephaly in the presence of *CEP55* mutation.

Materials and Methods

CEP55 messenger RNA Expression Analysis

CEP55 mRNA expression in human brain was extracted from the online database BrainSpan (<http://www.brainspan.org/>).⁽²⁰⁾ All data are publicly accessible via the Allen Brain Atlas data portal at www.developinghumanbrain.org. Human brain specimens from tissue collections of the Department of Neurobiology at Yale School of Medicine and the National Institute of Mental Health were used in that project. Brain tissues were not used if: a) aneuploidy or large scale chromosomal abnormalities were detected, b) malformations or lesions were present, c) neuron loss was found microscopically, d) cases tested positive for Hepatitis B, C or HIV, or e) maternal prenatal drug and/or alcohol abuse was reported. Depending on the stage of development different structures were dissected. mRNA was extracted and purified from the tissue and translated and enriched to cDNA by PCR. DNA sequencing was done on an Illumina Genome Analyzer II. Sequences were mapped to reference sequences and expression level of genes, exons, and spike-in RNAs were measured in RPKM (reads per kilobase of exon model per million mapped reads) using SAMtools and RSEQtools software packages.⁽²⁰⁾

For investigation of CEP55 mRNA expression, hybridization intensity was extracted from the metadata file "RNA-Seq Gencode v10 summarized to genes" for ages between 8 weeks gestation (the earliest age point) and adulthood. Data were graphed as mRNA expression as a function of age in each anatomical structure of interest including: striatum, lateral/medial ganglionic eminence, hippocampus, cerebellum / cerebellar cortex, amygdala, inferolateral temporal cortex, thalamus, occipital / visual cortex, and dorsolateral prefrontal cortex. Other structures are available for analysis in the BrainSpan database but were not used in this study.

Classification of certain structures in the Allen Brain Atlas made it difficult to show transcription over time. Some structures like the ganglionic eminences and neocortices had data only up until 10 weeks of development. To try to show the expression over all development, these data were combined with structures roughly equivalent to the early structures at a later developmental stage (e.g. the ganglionic eminences and the striatum).

Data were downloaded from the Allen Brain Atlas Transcriptome database and imported into an Excel file. Using Excel, the data were copied into other files based on structure of donor tissue. The data were then graphed using the Excel program showing mRNA expression in RPKM, as a function of age both prenatally and antenatally. The Excel program was also used to generate trendlines for CEP55 mRNA expression and to calculate average CEP55 expression across all BrainSpan data (included ungraphed data) at each time point.

Immunohistochemical Tissue Analysis

CEP55 protein localization was studied by immunohistochemistry using two commercial antibodies: a mouse IgG1 monoclonal anti-CEP55 (1/250 dilution Clone: EMRC10-11-55; eBioscience, San Diego CA) and a rabbit polyclonal IgG anti-CEP55 (1/250 dilution bs-7742R; Bioss, Woburn MA). A series of dilution and protocol variations was initially tested to optimize the antibody for use in human brain and kidney tissues. Formalin-fixed paraffin-embedded sections (5 μ m thick) of human brain previously derived from autopsies were treated using immunohistochemical methods. Normal brain tissues with no malformation, hemorrhage, or other pathological change including choroid plexus, cerebellum, brainstem, hippocampus, frontal cerebrum, and striatum from fetuses age 17, 19, 21, 23, 25, 31, and 40 weeks gestation, children age 2 weeks, 9 months, 2, 6, and 18 years, and adults age 40, 55, 75, and 84 years were used. Kidney tissue was studied at 22 and 29 weeks gestation and in a 6-week post-term birth infant. Samples of brain tissue from two of the affected fetuses (32 and 35 weeks gestation) along with age- and sex-matched control tissues were also studied. The third case had severe autolytic change related to in utero death; the tissue was not suitable for an immunohistochemical study.

Endogenous peroxidases were quenched using a 5% hydrogen peroxide in methanol solution for 10 min (to eliminate the high background staining caused by endogenous peroxidase activity on diaminobenzidine). Antigen retrieval was used to enhance labelling of CEP55 by heating slides in 0.01 M sodium citrate buffers pH 6.0 and 4.0, for the mouse and rabbit CEP55 antibodies respectively, for 20 minutes in a microwave facilitating antigen exposure for labelling. Primary antibodies underwent overnight incubation at 4°C for all immunostaining. This was followed by incubation with appropriate biotinylated secondary antibodies, followed by reaction with streptavidin-peroxidase, detection with diaminobenzidine (DAB, Sigma D5905), and finally counterstaining with hematoxylin. Negative controls were processed similarly without the primary antibody.

Results

The BrainSpan database data showed the highest levels of CEP55 mRNA expression in fetuses at 8 to 12 weeks gestation with a rapid decline reaching very low basal levels by 17 weeks, which persisted into adulthood. Structures with the highest expression included the ganglionic eminence (immature germinal tissue overlying the caudate nuclei in the frontal lobes), occipital cortex, and dorsolateral prefrontal cortex (Fig. 1). The lowest levels were seen in the cerebellum and inferolateral temporal cortex (Fig. 2). These were approximately 1/3 of the highest values seen in the other structures. Regions with high levels in normal brain correspond to the regions destroyed in the hydranencephaly brains.

The antibodies successfully stained the normal human brain and kidney tissues. In general, the mouse monoclonal antibody gave a stronger signal and less background, although there were some exceptions. In the 17-week fetuses, diffuse cytoplasmic immunoreactivity was identified in cerebellum (including the proliferative external granular zone), the neocortical region, and the ventricular zone and superficial region of the subventricular zone of the ganglionic eminence (Fig. 3a, 3d). This pattern persisted to 23 weeks. By 25 weeks both antibodies labelled radial glia in the ganglionic eminence (Fig. 3i). By 31 weeks neither antibody showed significant labelling in the cerebrum and

the sensitivity had reversed with the mouse antibody showing stronger labelling in the Purkinje layer of the cerebellum (Fig. 3c). By 40 weeks (term birth), immunoreactivity in the cerebellum expanded to include the molecular layer and scattered cells in the internal granular layer. This pattern persisted until old age (Fig. 3b). In certain regions such as the hippocampus, some neuron cell bodies were especially prominent (Fig. 3i). Labelling was generally weak in the white matter (Fig. 3h). Artery walls showed inconsistent labeling.

Brain tissue from the affected individuals showed strong labelling in the Purkinje neurons of the cerebellum and in the cerebral neuropil (Fig. 4c). Cerebellar staining was similar to the staining patterns seen in control brain tissues. In the cerebrum, labelling was less intense than that seen in normal brain tissue but localized to the multinucleate neurons (Fig. 4c,f).

CEP55 immunoreactivity in control kidney tissue was present in the cytoplasm of tubule cells throughout the cortex and medulla at 22 to 46 weeks post conception (Fig. 5a-c). The smaller distal convoluted tubules were always more intensely stained than the larger proximal tubules. The mouse and rabbit antibodies showed the same pattern, but the latter was less sensitive.

In neither normal nor pathological specimens was CEP55 immunoreactivity localized to cells with histologic features of mitosis. Discrete labelling corresponding to centrosomes, as has been shown in cultured cells, was never seen in these tissue samples.(8) However, the artifacts associated with autopsy material might make such fine localization impossible.

Discussion

CEP55 in Brain Development

The CEP55 mRNA expression data show that regions of brain with the highest expression in normal fetus from 8 to 16 weeks gestation, including the ganglionic eminences and occipital cortex, are subject to the most severe destruction in fetuses with mutated *CEP55*. Regions with lower expression, including the cerebellum and inferolateral temporal cortex, are relatively spared from the destructive process but contain abnormal multinucleated cells. If the mRNA expression correlates with protein levels, it suggests that regional differences in expression might also have dose-dependent functional roles. It should be noted that immunohistochemical detection of the protein persisted in some regions until old age in control tissue. This does not correlate well with the mRNA database, which indicates negligible expression in all brain regions after the fetal period. Immunohistochemical protein localization in human fetuses age 17 weeks onward indicate high levels of CEP55 in some germinal regions, but not exceeding levels in the stable cell populations. Although the destroyed brain regions correspond to the regions with normally high CEP55 mRNA expression, the cellular localization does not fully explain the pattern of damage.

Mechanisms of Hydranencephaly

The pathogenesis of hydranencephaly is poorly understood. Most authors postulate that it occurs as a consequence of vascular occlusion.(3) Three published cases of hydranencephaly had severely hypoplastic or absent internal carotid

arteries.(21–23) However, there have been documented cases of hydranencephaly with apparently normal intracranial vasculature.(24) This may represent either recanalization post occlusion or indicate a non-vascular pathogenesis. While the gross features of hydranencephaly in the Manitoba cases are similar to those seen with vascular abnormalities, the CEP55 protein analysis by immunohistochemistry did not show particular localization to blood vessels. As such, we postulate that the pathogenesis in hydranencephaly with renal dysplasia in homozygous *CEP55* mutation is due to non-vascular mechanisms and is related to the role CEP55 plays in cell cycle regulation.

Genetics of Hydranencephaly

A number of genetic associations with hydranencephaly have been described. In most of these cases, a specific etiology for the hydranencephaly has yet to be established and the associated phenotypes vary substantially between conditions. Like the CEP55 case, most cases of hydranencephaly with a known genetic component pathogenesis is thought to be non-vascular, with the exception of proliferative vasculopathy associated hydranencephaly.

In chromosomal changes such as triploid (XXY) karyotype, hydranencephaly has been seen in cases with and without mosaicism.(3,25) Genetic defects on chromosomes 7, 13, and 16 have been identified as harbouring genes responsible for severe hydranencephaly / microcephaly including chromosome 16 substitution 16p13.312.1 (26), deletion 7q- (27), deletion del(13)(q22) (28), and del(14)(q13q21).(29)

In two human conditions, a specific gene mutation has been described leading to hydranencephaly. X-linked hydranencephaly with abnormal genitalia is associated with mutation of the aristaless-related homeobox gene (*ARX*).(30) As a homeobox gene, *ARX* functions as a transcription factor thought to be involved in the development of many structures including the brain. Mutations in *ARX* have been associated with X-linked lissencephaly with abnormal genitalia, and agenesis of the corpus callosum. Human *ARX* is expressed at high levels in both dorsal and ventral telencephalon, including the neocortical ventricular zone and germinal zone of the ganglionic eminence, with less intense signals in the subventricular zone, cortical plate, hippocampus, basal ganglia and ventral thalamus.(31) *ARX* mutation in mice is associated with thinner cortical plate defects without any specific signs of apoptosis indicating a defect in cell proliferation.(32) Additionally, *ARX* mutant populations showed decreased GABAergic interneuron migration and differentiation in the embryonic forebrain. Thus, the hydranencephaly in *ARX* mutation occurs as a defect of cell proliferation and migration, rather than a cell cycle defect in *CEP55* mutation.

Hydranencephaly associated with Roberts syndrome is correlated to several mutations in *ESCO2*.(33) Roberts syndrome is an autosomal recessive developmental disorder, characterized by growth retardation, limb reduction, and craniofacial abnormalities including cleft lip and palate and a characteristic cytogenetic defect of centromere puffing, affecting most of the chromosomes in metaphase. Expression of *ESCO2* has been detected in the neuroepithelium of the hindbrain, midbrain, and telencephalic vesicle (forebrain). Mutation leads to defects in chromatid cohesion, subsequent mitotic spindle activation, and cell proliferation.(33) Thus, its pathogenesis to hydranencephaly is through a disruption at metaphase rather than presumed disruption at anaphase, in CEP55 mutation. Additionally, none of these human single gene disorders contain the multinucleated neurons characteristic of the Manitoba cases.

Animal Models of Brain Malformation and Multinucleated Neurons

Cytokinesis plays an important role in neurogenesis; in animal models, mutations of involved molecules have been shown to lead to hypoplastic brains. Zebrafish homozygous for a *CEP55* mutation that leads to a premature stop codon at residue 39 had cell cycle defects and exhibited brain destruction with edema, small eyes, jaw malformations, and increased larval mortality.(18) The heterozygotes showed no distinguishable differences from wildtype zebrafish. While the predicted cell cycle defects were noted in the homozygotes, the most striking aspect was the extensive apoptosis. Cell death was 2.2 times more extensive than in wildtype siblings. The authors postulated that CEP55 is necessary for regulation of Pi3k/Akt pathway, which is involved in cell cycle regulation and promotes cell growth and survival. Akt levels were severely depleted in homozygous mutants. In zebrafish, *akt1* knockdown has been reported to cause a decrease in neuronal progenitors.(34) Zebrafish CEP55 is 36% identical to human CEP55 with at least two of the three known phosphorylation sites conserved suggesting that the same phosphorylation sites are used in both zebrafish CEP55 and human CEP55. It is possible that the phenotypic changes seen in the zebrafish model represent a hydranencephaly-like malformation. The phenotypic changes in zebrafish provide a possible mechanism for apoptosis in the mutated human CEP55 homozygote cases.

Other animal models exhibit brain malformations with multinucleated neurons. *Flathead*, a neurological mutant in rats, is characterized by a flattened cranium, resting tremor, ataxia, progressive paralysis of the hind limbs, and early post-natal death. Multinucleated progenitor cells are present in ventricular and subventricular regions of the cortex and external granular layer of the cerebellum.(35) These regions associated with higher counts of multinucleated cells exhibit increased apoptosis. High levels of apoptosis leads to growth reduction among neuron populations of the cerebellum, neocortex, hippocampus, and retina.(36) The phenotype is due to a deletion mutation in the citron-kinase gene (Citron-K) and can be replicated in Citron-K knockout mouse models.(37,38) Citron-K disruption causes a significant change in the ratio of ventricular to abventricular cell divisions in the developing neocortex. (11) This suggests a decrease in the number of ventricular stem-like divisions and a corresponding increase in abventricular neuron cell divisions. Such a change could result in a premature depletion of progenitors and a corresponding decrease in the total number of neurons produced. (37) This suggests that a cytokinetic defect, without an increase in concurrent apoptosis, can lead to a phenotype of brain aplasia.

Renal Involvement in CEP55 Mutation

We were unable to identify multinucleate cells, an indicator of cytokinetic failure, in non-neural tissues. The underlying mechanism for renal dysgenesis and the limb dysmorphisms is unclear. It is possible that they relate to ciliary dysfunction given the connection between centrosomal proteins and ciliopathies such as nephronophthisis and Meckel-Gruber syndrome.(39) Ciliopathies are multisystem phenotypes that can include renal dystrophy, brain malformations, and polydactyly. They are associated with mutations in genes encoding components of the cilium and its anchoring structure.(40) During development, the primary cilia found in most vertebrate cells are instrumental in coordinating signal pathways and maintaining tissue homeostasis. Mutations in centrosomal proteins CEP83 and CSPP1 have been found to cause ciliopathies.(40,41)

It is possible that CEP55 may also play a similar role in ciliary anchoring. However, there is no published literature supporting this role for CEP55. It is also possible that the apoptotic mechanisms noted in zebrafish CEP55 mutants (18) might be responsible for the dysplastic kidney development. Currently, there remains a lack of published work describing a role for CEP55 in renal development, nor is there an animal model of CEP55 dysfunction in renal tissue. The stronger immunostaining of CEP55 in tubules of normal renal tissue and lack of staining in other kidney structures suggests a differential role for CEP55 in the kidney.

Cytologic localization and antibody details

It is unclear why staining patterns of CEP55 immunostaining did not differ between the brain tissue with mutated CEP55 and control tissues. Full-length human CEP55 recombinant protein was used to immunize BALB/c mice, and spleen cells were fused with NS-1 mouse myeloma cell line to generate the monoclonal mouse antibodies. Antibodies were screened with enzyme linked immunosorbent assay using recombinant CEP55 protein and Western blotting.(42) However, the target epitope for the monoclonal antibody has not been mapped (personal communication, Dr. Yoshihiko Hirohashi, December 2014). The peptide used to generate the polyclonal antibody was amino acids 155-210/464 within the protein. Given that the mutations in the Manitoba cases are predicted to cause truncation after amino acid position 425, a shortened abnormal protein product could be detected with the available antibodies. Additional knowledge of the monoclonal antibody epitope might help to explain the differences between the staining patterns of the monoclonal and polyclonal anti-CEP55 antibodies. We hypothesize that the mutation in *CEP55* altered the function of the protein product, but did not change the intracellular distribution of CEP55. There was no indication that the protein accumulates abnormally, which conceivably could have a toxic effect.

Limitations

Immunoblot (Western blot) using both CEP55 antibodies has yet to be done using tissue from the hydranencephalic cases. No frozen brain tissue is available although muscle tissue is. Future work will attempt to characterize the affinity of both CEP55 antibodies against mutated CEP55 tissue relative to CEP55 in control tissue. We anticipate that a protein of reduced molecular weight should be detected. Currently the affinity for CEP55 in mutated tissue using either of our antibodies is unknown. While our immunostaining results are similar in both mutated and non-mutated tissue and similar to brain staining patterns seen in other uses of these antibodies, we cannot be fully confident that our antibodies can fully detect the presence of truncated CEP55 in the case tissue we have used. Purified recombinant protein is commercially available (from OriGene), but is very expensive. It could be used to ensure that antibody binding to tissue is blocked by preabsorption.

Speculation on the Manitoba CEP55 Mutation Case

We speculate that cells in brain and kidney regions with a requirement for high levels of CEP55 cannot survive without normal expression of the protein, while cells with lower normal expression simply fail in cytokinesis (resulting in cells with multiple nuclei). Additional failure in ciliary anchoring and other apoptotic mechanisms may be present leading to the phenotype seen homozygous CEP55 mutation. All evidence points

towards a nonvascular etiology in the pathogenesis of hydranencephaly in these mutants.

Our data suggest CEP55 may be essential for the early development of the brain and kidney, but may not be as important in the formation of many other tissues, which are relatively spared. Persistent immunoreactivity in neuronal populations of the cerebrum and cerebellum after 31 weeks and into old age, as well as in the renal tubules, suggests that other non-mitotic functions likely exist. However, it is unclear based on the current literature what these functions might be.

Future Directions

Locally, we plan to do further characterization of the CEP55 antibodies using Western blots and available muscle tissue from the cases of the CEP55 homozygous mutations. Other work is needed to further elucidate phenotypes in animals with homozygous CEP55 mutations. A mouse knockout model might be helpful if the brain and renal abnormalities can be replicated. The International Mouse Strain Resource (IMSR) indicates that mouse embryonic stem cells, but not live mice, have been generated with CEP55 deletion. It may also be possible to deduce the expression patterns of CEP55 mRNA in developing renal tissue from a similar genetic atlas such as BrainSpan for renal tissue. This would additionally add information to the growing knowledge of the timing and role of CEP55 in the development of mammals and humans specifically.

References

1. Dixon A. Hydranencephaly. *Radiography*. 1988;54(163):12–3.
2. Stevenson, RE, Hall JG. Hydranencephaly. In: Stevenson, RE, Hall JG, editor. *Human Malformations and Related Anomalies*. Oxford University Press; 2006. p. 639.
3. Cecchetto G, Milanese L, Giordano R, Viero A, Suma V, Manara R. Looking at the missing brain: Hydranencephaly case series and literature review. *Pediatr Neurol*. 2013;48(2):152–8.
4. Bendon RW, Siddiqi T, de Courten-Myers G, Dignan P. Recurrent developmental anomalies: 1. Syndrome of hydranencephaly with renal aplastic dysplasia; 2. Polyvalvular developmental heart defect. *Am J Med Genet Suppl*. 1987;3: 357–65.
5. Gschwendtner A, Mairinger T, Soelder E, Alge A, Kreczy A. Hydranencephaly with renal dysgenesis: a coincidental finding? Case report with review of the literature. *Gynecol Obstet Invest*. 1997;44(3):206–10.
6. Hamby WB, Krauss RF, Beswick WF. Hydranencephaly; clinical diagnosis; presentation of 7 cases. *Pediatrics*. 1950;6:371-83.
7. Strauss, S, Bouzouki, M, Goldfarb, H, Uppal, V, Costales F. Antenatal ultrasound diagnosis of an unusual case of hydranencephaly. *J Clin Ultrasound*. 1984;12:420–2.
8. Chu, GC, Miller, WA, Norton, M, Kinney, HC, Genest, D, Folkerth RD. Hydranencephaly with Binucleate Neurons-Renal Dysplasia-Syndactyly syndrome in three siblings. *J Neuropathol Exp Neurol*. 1998;57(5):483.
9. Orton NC, Innes AM, Chudley AE, Bech-Hansen NT. Unique disease heritage of the Dutch-German mennonite population. *Am J Med Genet A*. 2008;146(8):1072–87.
10. Schweingruber C, Rufener SC, Zund D, Yamashita, A, Muhlemann O. Nonsense-mediated mRNA decay - mechanisms of substrate mRNA recognition and degradation in mammalian cells. *Biochem Biophys Acta*. 2013;(1829):612–23.
11. Chang YC, Wu CH, Yen TC, Ouyang P. Centrosomal protein 55 (Cep55) stability is negatively regulated by p53 protein through polo-like kinase 1 (Plk1). *J Biol Chem*. 2012;287(6):4376–85.
12. Martinez-Garay I, Rustom A, Gerdes H-H, Kutsche K. The novel centrosomal associated protein CEP55 is present in the spindle midzone and the midbody. *Genomics*. 2006;87(2):243–53.
13. Morita E, Sandrin V, Chung H-Y, Morham SG, Gygi SP, Rodesch CK, et al. Human ESCRT and ALIX proteins interact with proteins of the midbody and function in cytokinesis. *EMBO J*. 2007;26(19):4215–27.
14. Fabbro M, Zhou B-B, Takahashi M, Sarcevic B, Lal P, Graham ME, et al. Cdk1/Erk2- and Plk1-dependent phosphorylation of a centrosome protein, Cep55, is required for its recruitment to midbody and cytokinesis. *Dev Cell*. 2005;9(4):477–88.
15. Van Der Horst A, Simmons J, Khanna KK. Cep55 stabilization is required for normal execution of cytokinesis. *Cell Cycle*. 2009;8(22):3742–9.
16. Agromayor M, Martin-Serrano J. Knowing when to cut and run: mechanisms that control cytokinetic abscission. *Trends Cell Biol*. 2013;23(9):433–41.
17. Bastos RN, Barr FA. Plk1 negatively regulates Cep55 recruitment to the midbody to ensure orderly abscission. *J Cell Biol*. 2010;191(4):751–60.
18. Jeffery J, Neyt C, Moore W, Paterson S, Bower NI, Chenevix-Trench G, et al. Cep55 regulates embryonic growth and development by promoting Akt stability in zebrafish. *FASEB J*. 2015;1999–2009.
19. Jeffery J, Sinha D, Srihari S, Kalimutho M, Khanna KK. Beyond cytokinesis: the emerging roles of CEP55 in tumorigenesis. *Oncogene*. 2015;(February):1–8.
20. BrainSpan: Atlas of the Developing Human Brain [Internet]. Funded by ARRA Awards 1RC2MH089921-01, 1RC2MH090047-01, and 1RCMH089929-01. 2011. Available from: <http://developinghumanbrain.org>.
21. Kelly TG, Sharif UM, Southern JF, Gururajan K, Segall HD. An unusual case of hydranencephaly presenting with an anterior midline cyst, a posterior calcified mass, cerebellar hypoplasia and occlusion of the posterior cerebral arteries. *Pediatr Radiol*. 2011;41(2):274–7.
22. Stevenson DA, Hart BL, Clericuzio CL. Hydranencephaly in an infant with vascular malformations. *Am J Med Genet*. 2001;104(4):295–8.
23. Harwood-Nash DC. Congenital craniocerebral abnormalities and computed tomography. *Semin Roentgenol*. 1977;12:39–51.
24. Jordan L, Raymond G, Lin D, Gailloud P. CT angiography in a newborn child with hydranencephaly. *J Perinatol*. 2004;24(9):565–7.

25. Vecchi, C, Giovannucci-Uzielli ML, Donzelli GP, Seminara S, Gori A, Bini A, Scarlato C. Two new cases of triploidy in premature liveborn infants (author's transl). [in Ital Pediatr Med Chir. 1981;3:229–34.
26. Kavaslar GN, Onengüt S, Derman O, Kaya A, Tolun A. The novel genetic disorder microhydranencephaly maps to chromosome 16p13.3-12.1. *Am J Hum Genet.* 2000;66(5):1705–9.
27. McMorrow LE, Toth IR, Gluckson MM, Leff A, Wolman SR. A lethal presentation of de novo deletion 7q. *J Med Gen.* 1987;24(10):629–31.
28. Gershoni-Baruch R, Zekaria D. Deletion (13)(q22) with multiple congenital anomalies, hydranencephaly and penoscrotal transposition. *Clin Dysmorphol.* 1996;5(4):289–94.
29. Segawa Y, Itokazu N, Hirose A, Nakagawa S, Takashima S. A Case of Partial 14q- with Facial Features of Holoprosencephaly and Hydranencephaly. *Pediatr Neurol.* 2007;37(1):51–4.
30. Kato M, Das S, Petras K, Kitamura K, Morohashi KI, Abuelo DN, et al. Mutations of ARX Are Associated with Striking Pleiotropy and Consistent Genotype-Phenotype Correlation. *Hum Mutatn.* 2004;23(2):147–59.
31. Miura H, Yanazawa M, Kato K, Kitamura K. Expression of a novel aristaless related homeobox gene "Arx" in the vertebrate telencephalon, diencephalon and floor plate. *Mech Dev.* 1997;65(1-2):99–109.
32. Kitamura K, Yanazawa M, Sugiyama N, Miura H, Iizuka-Kogo A, Kusaka M, et al. Mutation of ARX causes abnormal development of forebrain and testes in mice and X-linked lissencephaly with abnormal genitalia in humans. *Nat Genet.* 2002;32(3):359–69.
33. Vega H, Trainer A H, Gordillo M, Crosier M, Kayserili H, Skovby F, et al. Phenotypic variability in 49 cases of ESCO2 mutations, including novel missense and codon deletion in the acetyltransferase domain, correlates with ESCO2 expression and establishes the clinical criteria for Roberts syndrome. *J Med Genet.* 2010;47(1):30–7.
34. Cheng Y-Z, Eley L, Hynes A-M, Overman LM, Simms RJ, Barker A, et al. Investigating embryonic expression patterns and evolution of AHI1 and CEP290 genes, implicated in Joubert syndrome. *PLoS One.* 2012;7(9):e44975.
35. Mitchell BD, Gibbons B, Allen LR, Stella J, D'Mello SR. Aberrant apoptosis in the neurological mutant Flathead is associated with defective cytokinesis of neural progenitor cells. *Dev Brain Res.* 2001;130(1):53–63.
36. Roberts MR, Bittman K, Li WW, French R, Mitchell B, LoTurco JJ, et al. The flathead mutation causes CNS-specific developmental abnormalities and apoptosis. *J Neurosci.* 2000;20(6):2295–306.
37. Sarkisian MR, Li W, Di Cunto F, Mello SRD, Loturco JJ. Citron-Kinase , a Protein Essential to Cytokinesis in Neuronal Progenitors , Is Deleted in the Flathead Mutant Rat. *J Neurosci.* 2002;22(8):1–5.
38. Di Cunto F, Imarisio S, Hirsch E, Broccoli V, Bulfone A, Migheli A, et al. Defective neurogenesis in citron kinase knockout mice by altered cytokinesis and massive apoptosis. *Neuron.* 2000;28(1):115–27.
39. Ferkol TW, Leigh MW. Ciliopathies: the central role of cilia in a spectrum of pediatric disorders. *J Pediatr.* 2012;160:366–71.
40. Shaheen R, Shamseldin HE, Loucks CM, Seidahmed MZ, Ansari S, Ibrahim Khalil M, et al. Mutations in CSPP1, encoding a core centrosomal protein, cause a range of ciliopathy phenotypes in humans. *Am J Hum Genet.* 2014;94(1):73–9.
41. Failler M, Gee HY, Krug P, Joo K, Halbritter J, Belkacem L, et al. Mutations of CEP83 Cause Infantile Nephronophthisis and Intellectual Disability. *Am J Hum Genet.* 2014;905–14.
42. Inoda S, Hirohashi Y, Torigoe T, Nakatsugawa M, Kiriya K, Nakazawa E, et al. Cep55/c10orf3, a tumor antigen derived from a centrosome residing protein in breast carcinoma. *J Immunother.* 2009;32(5):474–85.

Figures

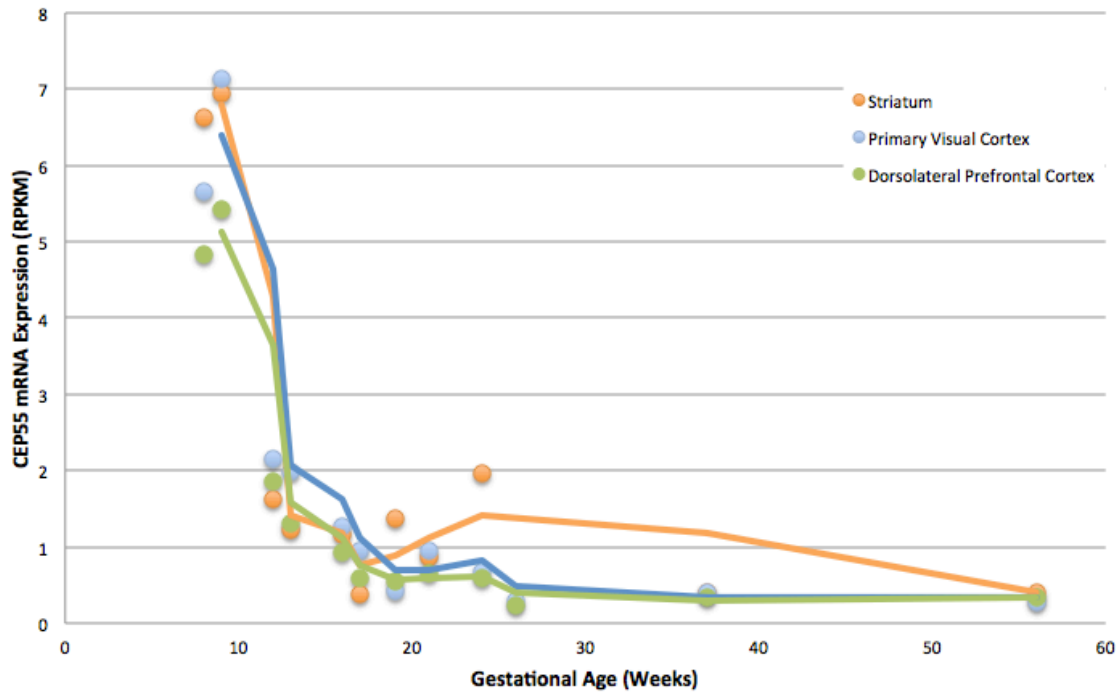


Figure 1: CEP55 mRNA expression in brain during fetal gestation and early infancy. These structures are destroyed in the brains of CEP55 mutants. Structures include striatum (designated as “caudal, medial and lateral ganglionic eminences” and “striatum” in BrainSpan database), primary visual cortex (designated as “occipital neocortex” and “primary visual cortex” in BrainSpan database) and dorsolateral prefrontal cortex. All data obtained from BrainSpan database.

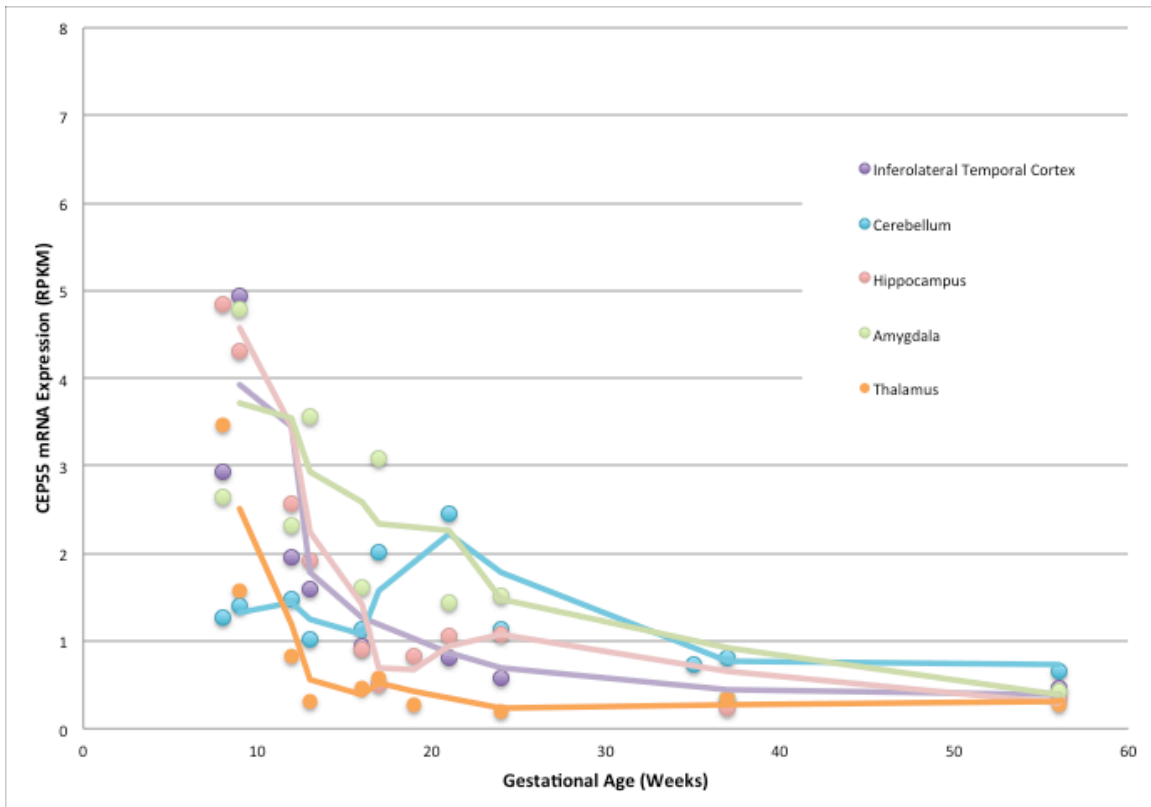


Figure 2: CEP55 mRNA expression in brain during fetal gestation and early infancy. These structures are relatively spared in the brains of CEP55 mutants. Structures include inferolateral temporal cortex (designated as “temporal neocortex” and “inferolateral temporal cortex” in BrainSpan database), cerebellum (designated as “upper rhombic lip”, “cerebellum” and “cerebellar cortex” in BrainSpan database), hippocampus, amygdala (“amygdaloid complex”) and thalamus (designated as “dorsal thalamus” and “mediodorsal nucleus of the thalamus” in BrainSpan database). All data obtained from BrainSpan database.

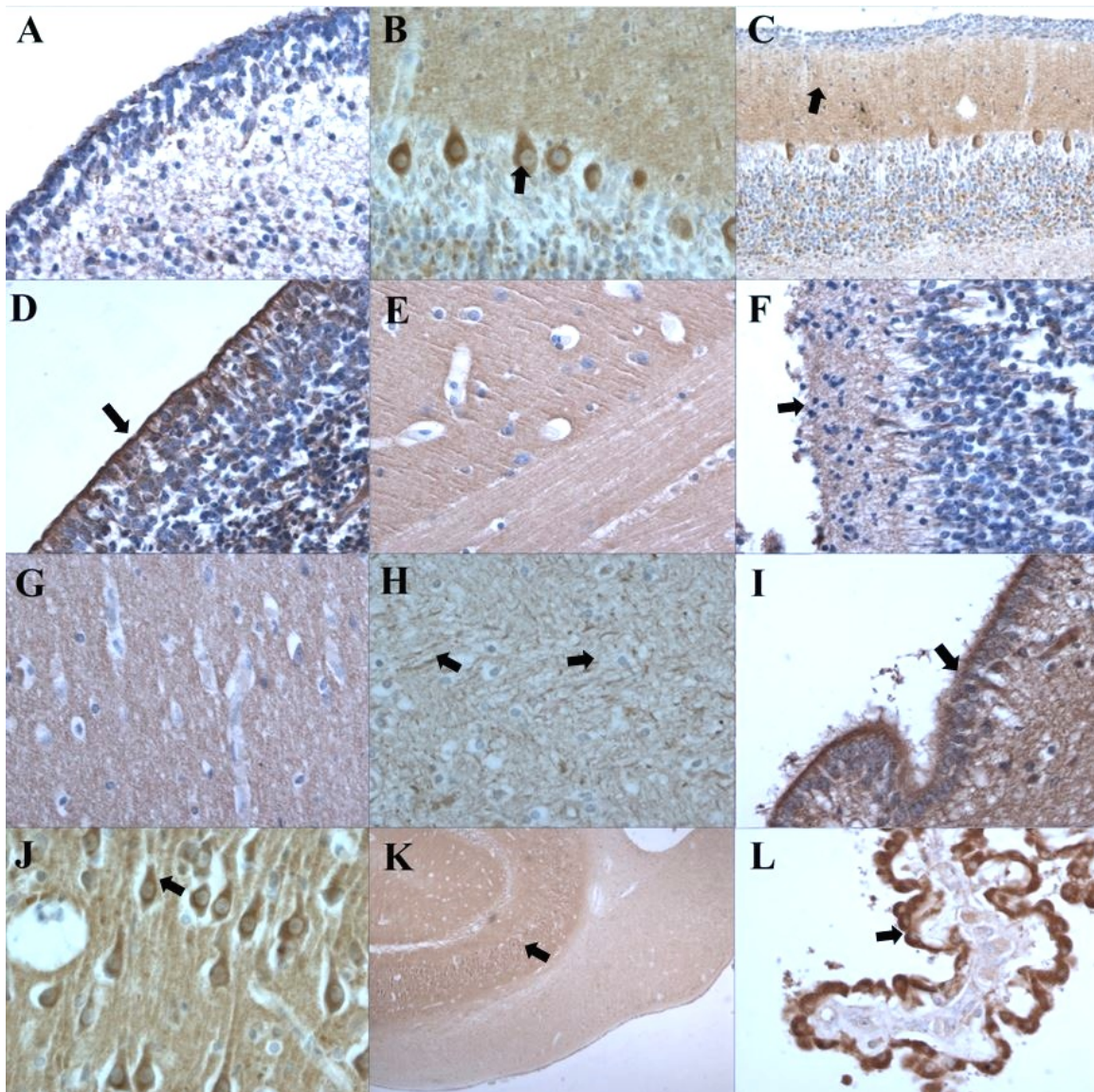


Figure 3: Immunohistochemical labelling of CEP55 (brown) with monoclonal mouse antibody (EMRC10-11-55) in paraffin-embedded control (normal) brain tissue. (A) External granular layer of cerebellum at 17 weeks gestation. Magnification 400x. (B) Cerebellum at 2 weeks after birth. A strongly labelled Purkinje neuron is indicated by a black arrow. Magnification 400x. (C) Cerebellum at 42 weeks. Arrow indicates the strongly labelled molecular layer, a feature that is present in tissue throughout adulthood. Magnification 200x. (D) Temporal germinal eminence at 17 weeks gestation. Strong apical labelling is shown by black arrow. Magnification 400x. (E) Striatum at 40 weeks gestation. Magnification 400x. (F) Developing neocortex at 19 weeks gestation. Black arrow indicates diffuse labelling in the subpial region. Magnification 400x. (G) White matter at 40 weeks gestation. Magnification 400x. (H) White matter at 75 years old. Black arrows highlight strongly labelled axons, thought to be due to axonal damage. Magnification 400x. (I) Midbrain at 25 weeks gestation. Black arrow shows strongly labelled ependymal cells in the cerebral aqueduct. Magnification 400x. (J) Hippocampal CA2 region at 2 weeks after birth. Black arrows highlight the strongly labelled pyramidal neurons. Magnification 400x. (K) Hippocampus at 2 weeks after birth. Black arrow indicates the strongly labelled CA2 region. Magnification 200x. (L) Choroid plexus at 9 months. Black arrow highlights strongly labelled choroid epithelial cells. Magnification 400x.

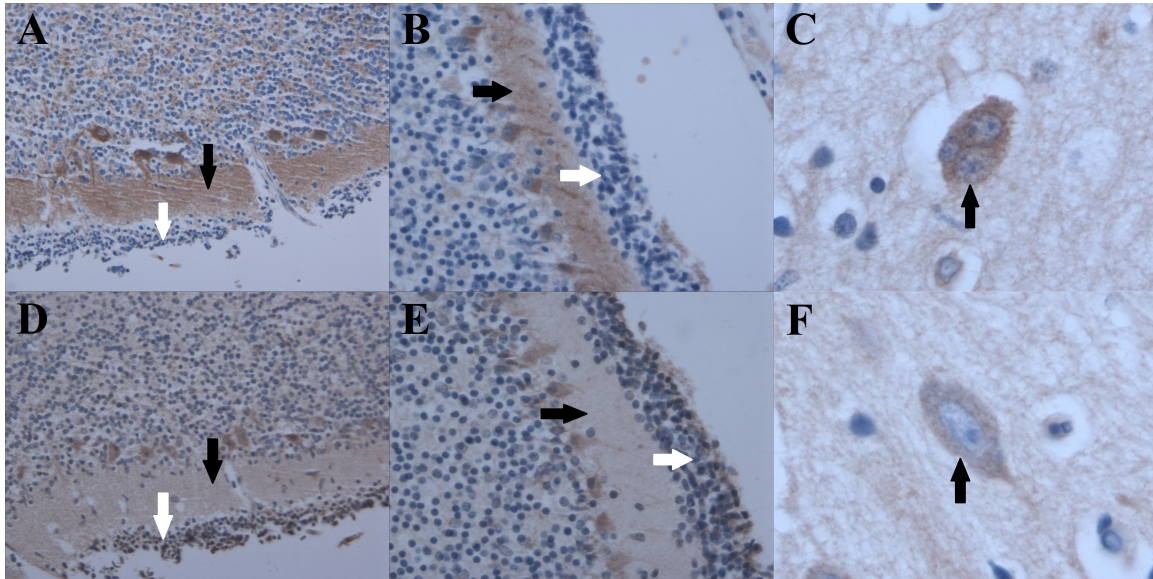


Figure 4: Immunohistochemical labelling of CEP55 (brown) in paraffin-embedded tissue (counterstained with hematoxylin blue). (A/D) Cerebellar tissue from 32 weeks gestation CEP55 mutant labelled with monoclonal mouse antibody and polyclonal rabbit antibody respectively. Molecular layer highlighted by black arrow. External granular layer indicated by white arrow. Magnification 400x. (B/E) Control cerebellar tissue at 32 weeks gestation stained with monoclonal mouse antibody and polyclonal rabbit antibody respectively. Molecular layer highlighted by black arrow. External granular layer indicated by white arrow. Magnification 400x. (C) Temporal cortex of CEP55 mutant stained with monoclonal mouse antibody. Strongly stained multinuclear neuron highlighted by black arrow. Magnification 400x. (F) Control temporal cortex at 32 weeks gestation stained with monoclonal mouse antibody. Strongly staining neuron indicated by black arrow. Magnification 400x.

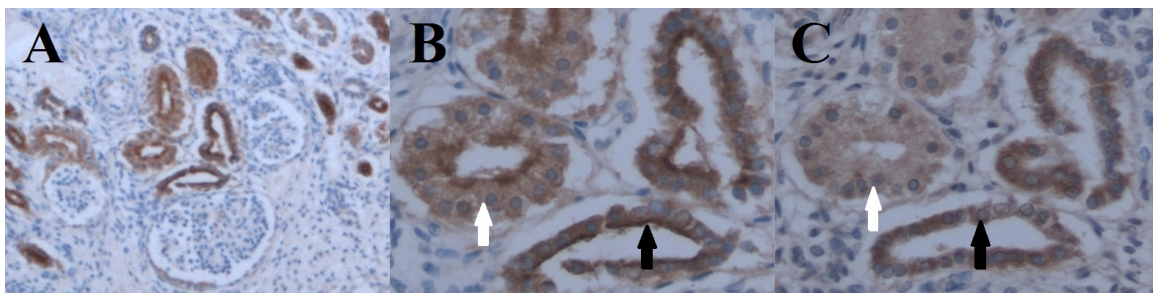


Figure 5: Immunohistochemical labelling of CEP55 (brown) in paraffin-embedded tissue (counterstained with hematoxylin blue). (A) Kidney tissue at 22 weeks gestation using monoclonal mouse antibody. Magnification 40x. (B/C) Kidney tissue at 22 weeks gestation using monoclonal mouse antibody and polyclonal rabbit antibody respectively. Strongly staining luminal edge of proximal tubules highlighted by black arrow, distal tubules highlighted by white arrow. Magnification 400x.